MATERIALS SCIENCE

Hydrogels of arrested phase separation simultaneously achieve high strength and low hysteresis

Guogao Zhang, Jason Steck, Junsoo Kim, Christine Heera Ahn, Zhigang Suo*

Hydrogels are being developed to bear loads. Applications include artificial tendons and muscles, which require high strength to bear loads and low hysteresis to reduce energy loss. However, simultaneously achieving high strength and low hysteresis has been challenging. This challenge is met here by synthesizing hydrogels of arrested phase separation. Such a hydrogel has interpenetrating hydrophilic and hydrophobic networks, which separate into a water-rich phase and a water-poor phase. The two phases arrest at the microscale. The soft hydrophilic phase deconcentrates stress in the strong hydrophobic phase, leading to high strength. The two phases are elastic and adhere through topological entanglements, leading to low hysteresis. For example, a hydrogel of 76 weight % water, made of poly(ethyl acrylate) and poly(acrylic acid), achieves a tensile strength of 6.9 megapascals and a hysteresis of 16.6%. This combination of properties has not been realized among previously existing hydrogels.

INTRODUCTION

A tendon consists of strong fibers and a soft matrix. The strong fibers bear loads, and the soft matrix transports water (*1*, *2*). The heterogeneous structure also enables the tendon to have excellent mechanical properties, such as high strength to sustain loads and low hysteresis to reduce energy loss (*2*). Biological tissues of heterogeneous structures have inspired the development of synthetic mimics (*3*). Hydrogels have been reinforced with polymer fibers (*4*), steel wires (*5*), glass fibers (*6*), and glass fabrics (*7*). Hydrogels of heterogeneous structures have been fabricated using techniques including three-dimensional printing (*8*), stereolithography (*9*), and sequential photolithography (*10*). Whereas the synthetic mimics have greatly expanded the property space of hydrogels, none have demonstrated simultaneous high strength and low hysteresis. Furthermore, they mimic the structures of biological tissues, not the process by which the biological tissues form the structures. Biological tissues form structures not by top-down processes but by self-assembly. It has been appreciated that self-assembly has the potential to synthesize heterogeneous materials of fine features and complex shapes at low cost (*11*, *12*).

Here, we describe a process that self-assembles hydrogels of heterogeneous structures (Fig. 1). The process begins with a hydrophobic polymer network, which is rubbery at room temperature (stage I). A precursor of a hydrophilic polymer network consists of monomers, cross-linkers, initiators, and water. Submerged in the precursor, the hydrophobic polymer network imbibes all ingredients of the precursor to form a gel of a single phase (stage II). When the monomers polymerize into a hydrophilic polymer network, the two networks interpenetrate, and separate into a water-rich phase and a water-poor phase (stage III). Submerged in pure water, the water-rich phase swells, and the water-poor phase stretches (stage IV). Because the hydrogel swells to equilibrium, the interpenetration keeps the network topology invariant, and arrests phase separation. The hydrogel has a microstructure of two length scales: polymer chains and polymer phases.

John A. Paulson School of Engineering and Applied Science, Harvard University, Cambridge, MA 02138, USA.
*Corresponding author. Email: suo@seas.harvard.edu

The thermodynamics of self-assembly is understood as follows. For hydrophilic polymers formed by radical polymerization, monomers are usually amphiphilic, consisting of a hydrophobic vinyl group, —CH═CH_2, and a hydrophilic group. The former enables radical polymerization, and the latter makes the polymers hydrophilic. For example, we synthesize a hydrogel with a hydrophobic polymer, poly(ethyl acrylate) (PEA), and a hydrophilic polymer, poly(acrylic acid) (PAAc). The AAc monomer is amphiphilic, consisting of the hydrophobic vinyl group, —CH═CH_2, and the hydrophilic carboxyl group, —COOH. In stage II, the AAc monomers bridge hydrophobic PEA polymers and water molecules, forming a PEA-AAc-water ternary phase. During polymerization, the hydrophobic vinyl groups of the AAc monomers react to form the backbones of PAAc polymers. A PAAc polymer consists of a carbon backbone and hydrophilic —COOH side groups. Such a polymer is no longer amphiphilic but hydrophilic. Furthermore, polymerization reduces the entropy of mixing. In stage III, both the energetic and entropic effects contribute to the polymerization-induced phase separation (*13*). The synthesis makes chemistry and topology antagonistic: The chemical dissimilarity of the two polymers separates the hydrogel into a water-rich phase and a water-poor phase, but the topological entanglements arrest phase separation (*14*). Both phases contain the hydrophilic and hydrophobic polymers, and the two phases adhere by entanglements. In stage IV, when submerged in pure water, the hydrogel imbibes more water, but the interpenetrating polymer network does not change the topology.

Hydrogels of heterogeneous structures have been self-assembled by physical interactions, such as ionic bonds (*15*), hydrogen bonds (*16*–*18*), and hydrophobic interactions (*19*). For such hydrogels, self-assembly is achieved by phase separation, producing a soft water-rich phase and a stiff water-poor phase. For example, in a poly(vinyl alcohol) (PVA) hydrogel, PVA chains form hydrogen bonds, and the water-poor phase is crystalline (*16*, *17*). In addition, we have previously studied phase separation in a hydrogel of poly(-methyl methacrylate) (PMMA) and PAAc (*19*). In the PMMA-PAAc hydrogel, PMMA chains are hydrophobic, and the water-poor phase is glassy. Despite having high strength, these hydrogels

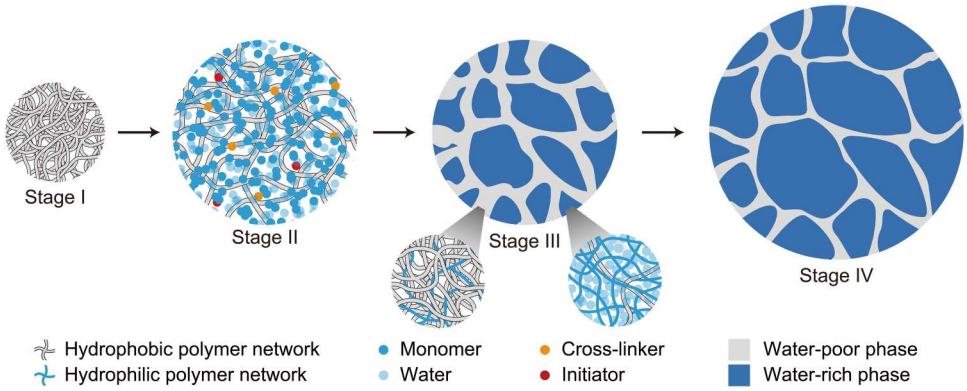

Fig. 1. The self-assembly of a hydrogel of heterogeneous structures. The process starts with a hydrophobic polymer network (stage I). The polymer network imbibes a precursor of a hydrophilic polymer network (stage II). The monomers in the precursor polymerize into a hydrophilic polymer network, which interpenetrates with the hydrophobic polymer network. The hydrogel separates into two phases, a water-rich phase and a water-poor phase. The phase separation is arrested at a microscale (stage III). When submerged in pure water, the water-rich phase swells, and the water-poor phase stretches (stage IV).

have pronounced hysteresis due to the inelastic deformation of the water-poor phase, which is either crystalline or glassy.

By contrast, here, we make the water-poor phase rubbery. The hydrophobic polymer chains cross-link into one network, and the hydrophilic polymers cross-link into another network. The two networks interpenetrate but do not form any covalent interlinks. After phase separation, the two phases are highly elastic and adherent, and the resulting hydrogel has high strength and low hysteresis. For example, a sample containing 76 wt % of water achieves a strength of 6.9 MPa and a hysteresis of 16.6%. Strength is measured by stretching a sample to rupture (Fig. 2A), and hysteresis is measured by stretching and releasing a sample (Fig. 2B). Here, we report hysteresis at a maximum stretch of 2. The PEA-PAAc hydrogel is compared with existing hydrogels on the plane of strength and hysteresis (Fig. 2C). The PEA-PAAc hydrogel occupies the top left corner of the plane. Such a hydrogel of simultaneous high strength and low hysteresis has not been realized before. As we will show, it is phase separation, rather than interpretation of the polymer networks, that strengthens the hydrogel. We further show that this method of synthesizing hydrogels of arrested phase separation is general and is readily extended to many other combinations of polymers.

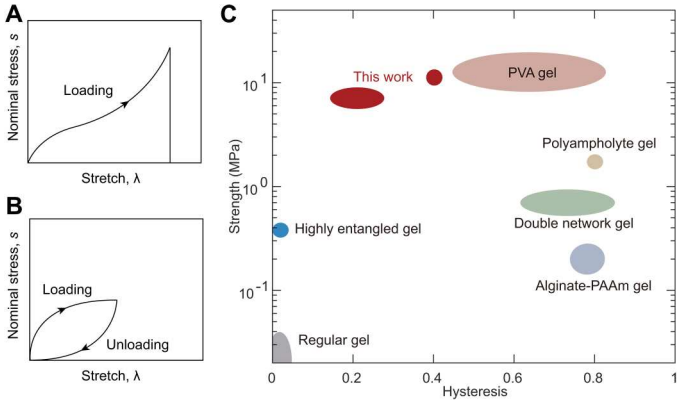

Fig. 2. The strength and hysteresis of representative hydrogels. (**A**) Define the nominal stress, *s* as the applied force divided by the undeformed cross-sectional area; the stretch, λ as the deformed length divided by the undeformed length; and the strength as the nominal stress at rupture. (**B**) Hysteresis is defined as the ratio of two areas: the area enclosed by the stress-stretch curves of loading and unloading and the area under the stress-stretch curve of loading. (**C**) Hydrogels are compared on the strength-hysteresis plane. Load-bearing applications often require hydrogels of high strength and low hysteresis (the shaded region), but it has been a challenge to synthesize hydrogels to achieve both simultaneously. PVA hydrogel, poly(vinyl alcohol) hydrogels; alginate-PAAm gel, alginate-poly(acrylamide) gel. (*15*, *17*, *20*, *22*, *23*).

RESULTS

We choose PEA as a model hydrophobic polymer for two reasons: low interchain friction and low entanglement molecular weight. The low interchain friction leads to an elastomer of low hysteresis of 7.7% (*20*). The low entanglement molecular weight is such that, along a PEA chain, two nearby entanglements on average are separated by only 120 repeat units (*21*). For a sample with a cross-linker–to-monomer molar ratio, $C = 10^{-4}$, each PEA chain between two cross-links on average has $(2C)^{-1} = 5000$ repeat units. Consequently, in PEA, the entanglements greatly outnumber cross-links. The dense entanglements enable PEA to be made with extremely long polymer chains but still with adequate elastic modulus. The long polymer chains make PEA strong, tough, and fatigue-resistant (*20*).

A PEA network is hydrophobic but imbibes liquid monomers for hydrogels. We have tested four liquid monomers for hydrogels, and confirmed that PEA imbibes every one of them (fig. S1). Thus, each is a valid choice to self-assemble a hydrogel of heterogeneous structures. Here, we choose AAc monomer as a demonstration. PEA can imbibe a large amount of AAc. To avoid excessive swelling, we submerge PEA in an aqueous solution of AAc. The amphiphilic AAc monomers act as bridges between the hydrophobic PEA chains and water molecules, so that PEA imbibes both AAc and water, and the swelling ratio is controlled by the water-to-AAc molar ratio, *W*. In this work, the swelling ratio is calculated as the weight ratio of samples before and after swelling.

The synthesis of PEA-PAAc hydrogel consists of four stages (Fig. 3A). Films of PEA are prepared by radical polymerization of ethyl acrylate (stage I). When a PEA film is submerged in an AAc-water solution with $W = 2$, PEA swells and forms a PEA-AAc-water

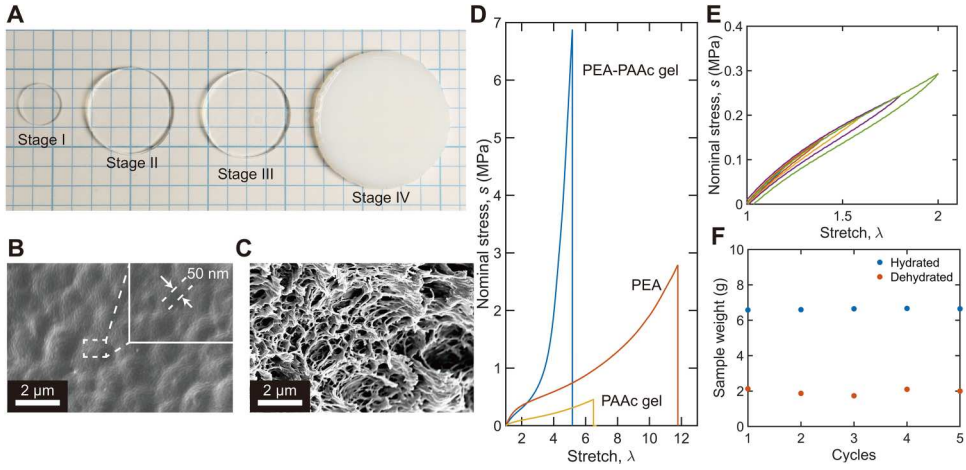

Fig. 3. PEA-PAAc hydrogel. (**A**) Photos of the poly(ethyl acrylate)–poly(acrylic acid) (PEA-PAAc) hydrogel in the four stages of synthesis. Scanning electron microscopy images of the PEA-PAAc hydrogel in stage III (**B**) and stage IV (**C**). The images are taken after the samples are freeze-dried. (**D**) Stress-stretch curves of the PEA-PAAc hydrogel, PEA elastomer, and PAAc hydrogel. (**E**) Stress-stretch curves under loading and unloading of the PEA-PAAc hydrogel with different rangers of stretch. (**F**) The PEA-PAAc hydrogel is repeatedly hydrated in pure water at 25°C to equilibrium and then dehydrated at 65°C for 1 hour. The weights of hydrated and dehydrated samples are recorded.

ternary phase (stage II). The AAc-water solution also contains small amounts of cross-linker and initiator. Under an ultraviolet (UV) lamp, the AAc monomers polymerize and cross-link into a PAAc network, resulting in a PEA-PAAc interpenetrating network (stage III). Submerged in pure water, the sample swells to equilibrium (stage IV). The sample is transparent in stage I to stage III but translucent in stage IV.

Samples in stage III and stage IV are freeze-dried and imaged using a scanning electron microscope. The sample does not show a clear porous structure in stage III (Fig. 3B) but is clearly porous in stage IV (Fig. 3C). The feature size is ~50 nm in stage III and ~400 nm in stage IV. These feature sizes are consistent with the observation that the sample is transparent in stage III but translucent in stage IV. The images also suggest that phases separate in stage III. The water-rich phase contains mostly hydrophilic polymer PAAc, and the water-poor phase contains mostly hydrophobic polymer PEA. When the stage III sample is submerged in pure water, the former swells, and the latter stretches. Because both polymer networks are cross-linked, the swelling keeps the topology of the interpenetrating network invariant. The PEA-PAAc hydrogel contains 5.3 wt % PEA, 19.1 wt % PAAc, and 75.6 wt % water.

We next study the mechanical properties of the stage IV sample. For comparison, we also prepare a pure PEA elastomer and a pure PAAc hydrogel, each with a cross-linker–to-monomer ratio, $C = 10^{-4}$. The PAAc hydrogel contains 79.9 wt % water, comparable to that in the PEA-PAAc hydrogel. The PEA-PAAc hydrogel, PEA elastomer, and the PAAc hydrogel are all stretched until rupture (Fig. 3D). The initial slope of the stress-stretch curve defines the modulus, which is 443 kPa for the PEA-PAAc hydrogel, 592 kPa for the pure PEA elastomer, and 161 kPa for the pure PAAc hydrogel. The nominal stress at rupture defines the strength, which is 6.9 MPa for the PEA-PAAc hydrogel, 2.8 MPa for the pure PEA elastomer, and 0.46 MPa for the pure PAAc hydrogel. The statistical scatters of these properties are summarized in table S1. The strength of the PEA-PAAc hydrogel is unexpectedly high. The PEA-PAAc hydrogel contains 5.3 wt % PEA and 94.7 wt % PAAc hydrogel. The strength of the PEA-PAAc hydrogel determined by the rule of mixture is ~0.58 MPa, which is more than 10 times lower than the measured strength of the PEA-PAAc hydrogel. The high strength of the PEA-PAAc hydrogel is demonstrated by stretching it (movie S1) and using it to lift a gallon (3.8 liters) of water (movie S2). Note that the stretchability of PEA-PAAc hydrogel is lower than both pure PEA and pure PAAc. A likely reason is that the PEA network in the PEA-PAAc hydrogel has been prestretched twice during the preparation of the hydrogel, once at stage II where the PEA network is swollen in the AAc-water solution, and the other time at stage IV where the sample is submerged in water to swell to equilibrium.

On loading and unloading, the PEA-PAAc hydrogel shows low hysteresis (Fig. 3E). The hysteresis is 7.7% for the PEA elastomer (fig. S2) and 16.6% for the PEA-PAAc hydrogel. The PEA-PAAc hydrogel has higher hysteresis than the PEA elastomer but has much lower hysteresis than existing tough hydrogels, which are usually greater than 70% (*15*, *22*–*24*). The PEA-PAAc hydrogel also has low hysteresis at a large stretch (>2; fig. S3). Our hydrogel has a value of hysteresis similar to that of load-bearing tissues, such as tendons (*25*). The toughness of the PEA-PAAc hydrogel is ~1700 J m^{-2} (fig. S4), which is similar to that of the PEA elastomer (*20*).

After a stage IV sample is placed in an oven at 65°C for 1 hour, the sample partially dehydrates and approaches the weight of a stage III sample. After submerging the dehydrated sample in pure water at room temperature overnight, the sample swells and recovers the weight of a stage IV sample. We repeat dehydration and swelling five times, and the sample changes weight repeatedly between that of stage III and stage IV (Fig. 3F). The sample also becomes transparent and opaque cyclically.

We now conduct additional experiments to understand the high strength of the PEA-PAAc hydrogel. Because the PEA-PAAc hydrogel is much stronger than both PAAc hydrogel and PEA elastomer, the high strength of the PEA-PAAc hydrogel can only come from the synergy of the PEA network and PAAc network, which

interpenetrate through topological entanglements and separate into two phases.

We first demonstrate that interpenetration of two polymer networks alone does not lead to high strength; rather, phase separation leads to the high strength of the PEA-PAAc hydrogel. Water, PEA, and PAAc are soluble in *N*,*N*′-dimethylformamide (DMF). We submerge a stage IV PEA-PAAc hydrogel into a large amount of DMF for 1 day. DMF migrates in and water migrates out, resulting in a PEA-PAAc organogel. The organogel weighs much more than the hydrogel. We then evaporate DMF from the organogel until the organogel has the same weight as the stage IV hydrogel. Whereas the hydrogel separates into phases and is opaque, the organogel does not separate into phases and is transparent (Fig. 4A). The stage IV hydrogel and the organogel have the same swelling ratio and the same interpenetrating network. Consequently, the differences in their mechanical properties result from phase separation. The organogel has the same stretchability as the hydrogel (λ ~5.2) but has strength about 10 times lower than the hydrogel (Fig. 4B).

We further demonstrate that PEA in the PEA-PAAc hydrogel bears most of the load. We prepare PEA-PAAc hydrogels with varying volumetric fraction of PEA, ϕ_{PEA}, by drying the stage IV sample. ϕ_{PEA} is calculated as the inverse of the swelling ratio, neglecting the small difference in the density of PEA, PAAc, and water. The stage IV sample has the lowest $\phi_{PEA} = 0.06$. We then cut the dog bone–shaped samples from these gels and uniaxially stretch them until rupture (Fig. 4C). The rupture stretch decreases with swelling.

The PEA network in the PEA-PAAc hydrogel is stretched both by swelling and applied force. The length in the deformed state divided by the length of the pure PEA is $\lambda\varphi_{PEA}^{-1/3}$, and the applied force divided by the cross-sectional area of the pure PEA is $s\varphi_{PEA}^{-2/3}$. These quantities are used to replot the stress-stretch curves (Fig. 4D). The curves for various values of ϕ_{PEA} collapse onto each other when $\lambda\varphi_{PEA}^{-1/3} < 7$, demonstrating that the PEA carries most of the load during extension. Furthermore, the maximum values of $\lambda\varphi_{PEA}^{-1/3}$ for all ϕ_{PEA} collapse to ~13. This stretch is approximately equal to the theoretical stretchability of the PEA network (Supplementary Text 1). This suggests that the rupture stretch of the PEA-PAAc hydrogel is determined by the PEA network. The normalized strengths when $\phi_{PEA} = 0.06$ and 0.1 are approximately the same and are as high as ~45 MPa. The normalized strengths when $\phi_{PEA} = 0.12$ and 0.16 are lower than the normalized strengths when $\phi_{PEA} = 0.06$ and 0.1. The difference is not understood at this writing.

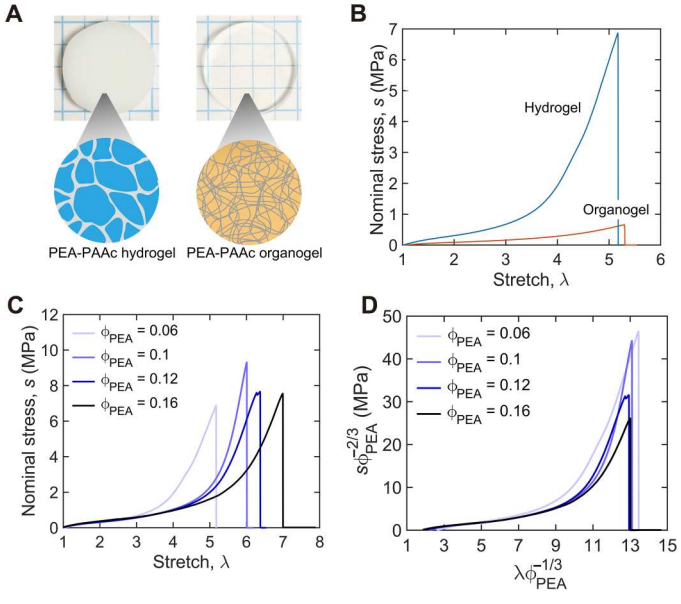

Fig. 4. PEA-PAAc hydrogel and PEA-PAAc organogel. (**A**) Whereas stage IV PEA-PAAc hydrogel separates into phases and is opaque, the PEA-PAAc organogel does not separate into phases and is transparent. (**B**) The PEA-PAAc hydrogel and organogel are stretched until rupture. (**C**) The stress-stretch curves of the PEA-PAAc hydrogels with varying volumetric fraction of PEA, ϕ_{PEA}. (**D**) The stress-stretch curves are replotted using $\lambda\varphi_{PEA}^{-1/3}$ and $s\varphi_{PEA}^{-2/3}$.

The PEA network in the pure PEA and the PEA-PAAc hydrogel has strengths of ~2.8 and ~45 MPa, respectively. We interpret this large difference in terms of stress deconcentration. We observe flaws with a size of ~10 μm on the edge of the samples and no larger flaws in the samples (fig. S5). Because the flaw size is smaller than the fractocohesive length of PEA-PAAc hydrogel (Supplementary Text 2), these flaws do not affect the strength (*26*–*28*). Because the two phases interpenetrate and the PEA-rich phase (i.e., water-poor phase) is much stiffer than the PAAc-rich phase (i.e., water-rich phase), the stress at a crack tip distributes over the PEA-rich phase. By contrast, the PEA elastomer does not separate into phases, so that the stress at the crack tip distributes over individual PEA chains. The PEA-rich phase in the PEA-PAAc hydrogel is several orders of magnitude larger than the PEA chain in the PEA elastomer, so the stress at crack tip is less concentrated in the PEA-PAAc hydrogel. Through stress deconcentration, the load-bearing capacity of each individual PEA chain in the PEA-PAAc hydrogel is much higher than those in the PEA elastomer.

The rupture force of a C—C bond is a few nanonewtons, e.g., 2 nN (*29*, *30*), and the area per monomer is 2.2×10^{-19} m^2, giving the theoretical strength of C—C bond of 9×10^9 Pa. This covalent bond strength, however, is orders of magnitude higher than the strength of a polymer network. This fact has been noted before (*26*). A possible mechanism has been analyzed recently (*31*). The covalent bond energy is several electrons volts, and the thermal energy is on the order of k_BT = 1/40 eV at room temperature, where k_B is the Boltzmann constant and T is the absolute temperature. The two types of energy differ by about two orders of magnitude. The force-stretch curve of a polymer chain is *J* shaped. Before the chain is pulled near rupture, the chain only carries the entropic force, which is low. The force approaches the covalent bond force when the chain is near rupture. A polymer network has polymer chains with different numbers of links per chain. When the network is stretched near rupture, only a small fraction of the polymer chains are stressed to the covalent bond strength, and the majority of polymer chains still carry entropic forces.

The PEA elastomer swells differently in hydrogel precursors with different W (fig. S6). AAc is a good solvent for PEA, but water is a poor solvent. As a result, the swelling ratio of stage II increases as W decreases. When $W \leq 1$, the swelling ratio of PEA is constant, suggesting that the swelling ratio is limited by the cross-links of the PEA network. Changing the swelling ratio in stage II changes the composition of the stage IV hydrogel. For example, when $W = 4$, the resulting stage IV hydrogel contains 25.8% PEA, 14.9% PAAc, and 59.3% water. The hydrogel is opaque, which

indicates the phase separation (fig. S7). The mechanical properties are also affected by changing W. When $W = 4$, the strength is 1.2 MPa, the elastic modulus is 447 kPa, and the hysteresis is 16.6%.

As we noted before, this method of synthesizing hydrogels of arrested phase separation is readily extended to many other combinations of polymers (fig. S1). Here, we choose a commercial thermoplastic elastomer, PEBAX, as a hydrophobic elastomer. PEBAX is a block copolymer with crystalline rigid polyamide blocks and soft polyether blocks and has excellent mechanical properties and biocompatibility (*32*). The rigid blocks serve as physical cross-links for PEBAX. We use an AAc-water solution with $W = 4$ as the hydrogel precursor. The stage IV PEBAX-PAAc hydrogel contains 18.3 wt % PEBAX, 18.6 wt % PAAc, and 63.1 wt % water. A strip of the PEBAX-PAAc hydrogel, 10 mm wide and 1 mm thick, can lift a weight of ~15 pounds (6.8 kg) (Fig. 5A). The resulting PEBAX-PAAc hydrogel shows an elastic modulus of ~1.34 MPa, strength of ~10 MPa, and stretchability of ~8.5 (Fig. 5B). Despite its high water content, the PEBAX-PAAc hydrogel has impressive mechanical properties compared to those of the pure PEBAX elastomer (fig. S8). In cyclic loading, the PEBAX-PAAc hydrogel and pure PEBAX have comparable hysteresis (Fig. 5C). The PEBAX-PAAc hydrogel has a compressive strength of >1 GPa (fig. S9) and toughness of ~9200 J m^{-2} (fig. S10).

We have shown phase separation leads to high strength. However, phase separation without arrest leads to materials of unstable microstructures. Here, we arrest phases through cross-linking the PEA elastomer and PAAc hydrogel. Without cross-links, the individual polymer chains can migrate over long distances and coarsen the phases. In the PEBAX-PAAc hydrogels, the crystalline rigid domains in PEBAX function as cross-links.

The tailoring of the hydrophobicity of polymeric networks has been an effective way to change the properties of a hydrogel (*33*, *34*). For example, a nonswellable hydrogel can be prepared by a single network of block copolymers of hydrophilic and hydrophobic segments. Such a hydrogel has not only low hysteresis but also low strength of ~100 kPa (*35*). Interpenetrating networks of hydrophobic polymers and hydrophilic polymers have been prepared, but none of the previous studies have reported unusual mechanical properties (*36*–*39*). The work presented here demonstrates a general method to make hydrogels of high strength and low hysteresis.

DISCUSSION

A hydrogel of heterogeneous structures can be self-assembled using a mixture of hydrophobic and hydrophilic polymers. We have demonstrated that such a hydrogel simultaneously achieves high strength and low hysteresis. The hydrophobic network and hydrophilic network do not interlink by chemical bonds but interpenetrate by topological entanglements. The synthesis makes chemistry and topology antagonistic: The chemical dissimilarity of the two polymers separates the hydrogel into a water-rich phase and a water-poor phase, but topological entanglements of the two networks arrest the phase separation. The two phases are elastic and adhere strongly through topological entanglements, so that the hydrogel has low hysteresis. The water-rich phase is much softer than the water-poor phase, so that the latter bears most of the load when the hydrogel is stretched. The large difference in the moduli of the two phases enables the water-rich phase to deconcentrate stress in the water-poor phase. It is the separation of phases, rather than the interpenetration of polymer networks, that strengthens the hydrogel. The hydrogel outperforms existing hydrogels in terms of the combination of high strength and low hysteresis. It is hoped that hydrogels of arrested phase separation will aid in bioengineering and soft robotics.

MATERIALS AND METHODS

Preparation of PEA

Ethyl acrylate (EA; E9706), *N*,*N*′-methylenebisacrylamide (MBAA; M7279), 2-hydroxy-4′-(2-hydroxyethoxy)-2-methylpropiophenone (Irgacure 2959; 410896), and DMF (227056) were purchased from Sigma-Aldrich and used as received. The PEA precursor was prepared by mixing EA, MBAA, and Irgacure 2959 with an MBAA-AAc molar ratio of $C = 10^{-4}$ and an Irgacure 2959–AAc molar ratio of 4×10^{-5}. A mold was made of a silicone sheet (McMaster, 1460N11) as a spacer and a glass plate (McMaster, 8476K15) as a substrate. The precursor was then poured onto the mold and sealed with another glass plate. The mold and the glass plate were fixed by binder clips and placed in a polyethylene zip bag (VWR, 4662002). The bag was pressed to remove air, zipped, and irradiated with UV light (15 W, 365 nm; UVP XX-15L) for at least 6 hours. The obtained sample was removed from the mold and placed in a hood for 24 hours to evaporate the unreacted monomers.

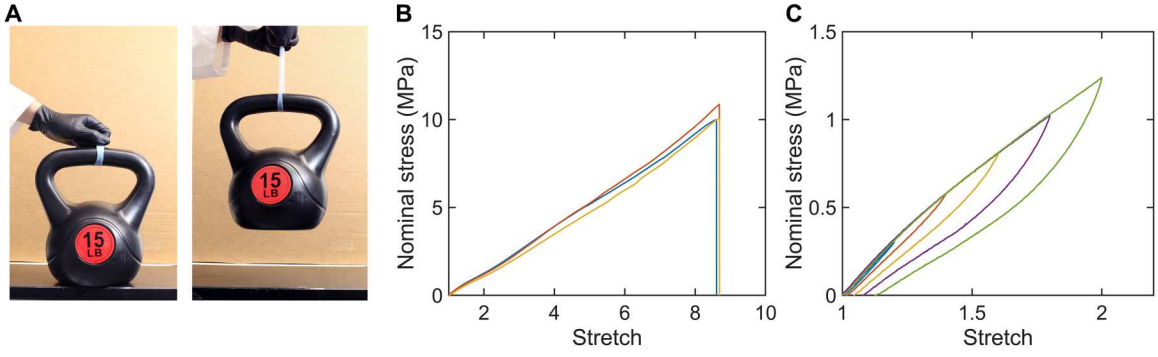

Fig. 5. PEBAX-PAAc hydrogel. (**A**) Photo of the PEBAX-PAAc hydrogel hanging a weight. (**B**) Stress-stretch curves of the PEBAX-PAAc hydrogel. (**C**) Stress-stretch curves under loading and unloading of the PEBAX-PAAc hydrogel with different rangers of stretch.

Preparation of PEA-PAAc hydrogel

AAc (147230) was purchased from Sigma-Aldrich and used as received. Deionized water was purchased from Poland Spring. The hydrogel precursor was a solution prepared by mixing water, AAc, MBAA, and Irgacure 2959 with a fixed MBAA-AAc molar ratio of $C = 10^{-4}$ and an Irgacure 2959–AAc molar ratio of 4×10^{-5} but different water-AAc molar ratios W ranging from 0 to 5. PEA films were swollen in the hydrogel precursor to equilibrium and were kept in darkness. The swollen sample (stage II) was taken out from the precursor, wiped with tissues, held between two glass slides, fixed by binder clips, and placed into a polyethylene zip bag (VWR, 4662002). The bag was pressed to remove air, zipped, and irradiated with UV light for at least 6 hours. The obtained sample (stage III) was submerged in pure water to swell to equilibrium at room temperature.

Preparation of PAAc hydrogel

The hydrogel precursor solution was prepared by mixing water, AAc, MBAA, and Irgacure 2959 with an MBAA-AAc molar ratio of $C = 10^{-4}$, an Irgacure 2959–AAc molar ratio of 4×10^{-5}, and a water-AAc molar ratio $W = 2$. The precursor was then poured onto the mold and sealed with another glass plate. The mold and the glass plate were fixed by binder clips and placed in a polyethylene zip bag. The bag was pressed to remove air, zipped, and irradiated with UV light for at least 6 hours. The obtained sample was removed from the mold and submerged in pure water to swell to equilibrium at room temperature. Water was then removed from the fully swollen sample by evaporation to control its water content.

Preparation of PEBAX-PAAc hydrogel

PEBAX 2533 pellets were purchased from Arkema. The PEBAX film was prepared by hot pressing the pellets at 180°C for 5 min. The hydrogel precursor solution was prepared by mixing water, AAc, MBAA, and Irgacure 2959 with an MBAA-AAc molar ratio of $C = 10^{-4}$, an Irgacure 2959-AAc molar ratio of 4×10^{-5}, and a water-AAc molar ratio $W = 4$. PEBAX film was swollen in the hydrogel precursor to equilibrium and was kept in darkness. The swollen sample was taken out from the precursor, wiped with tissues, held between two glass slides, fixed by binder clips, and put into a polyethylene zip bag. The bag was pressed to remove air, zipped, and irradiated with UV light for at least 6 hours. The obtained sample was submerged in pure water to swell to equilibrium at room temperature.

Tensile tests

The samples were cut into a dumbbell shape by a die cutter (Ace Steel Rule Dies, ISO 527-2-5B), and tested by an Instron 5966 machine with a 100-N load cell. During stretching, the force F and the displacement L_D were recorded. The samples were stretched monotonically until rupture, and the stretch rate was fixed at 1 mm s^{-1} unless otherwise noted. The elastic modulus was obtained from the slope of the stress-stretch curve in the linear elastic region (stretch of <1.05).

Toughness tests

Grippers were made of acrylic sheets (McMaster, 8560K172). Two samples were cut into a rectangular shape of 7 cm by 3 cm, and glued with the grippers using Krazy Glue. The resulting sample has a free area of 7 cm by 1 cm. One sample was cut at the edge of the sample to form a ~5-mm crack with a razor blade, and the other one remains intact. The intact one was loaded on the Instron 5966 with a 10-kN load cell and monotonically stretched until break. The stretch and stress were recorded. The elastic energy density function $w(\lambda)$ was calculated by integrating the stress-stretch curve until stretch λ. The sample with a crack was then monotonically stretched until rupture, and the stretch λ_{max} when the crack started to propagate was recorded. The toughness is calculated as $w(\lambda_{max})H$, where H is the height of the sample.

Compressive tests

The samples were cut into a round shape with a diameter of ~3 mm by a puncher (McMaster, 3424A12) and tested by Instron 5966 with a 10-kN load cell. The samples were compressed monotonically, and the rate was fixed at 0.001 s^{-1}.

Scanning electron microscopy

The images were conducted using a Zeiss Ultra Plus Field-Emission SEM. All the samples were freeze-dried for 3 days before tests. All the samples were first immersed in liquid nitrogen for 1 min and then broken to expose the cross section. The cross section was then coated with a 5-nm-thick Pt/Pd layer using a metal sputter coater (208HRD, Cressington Scientific Instruments) and imaged.

Supplementary Materials

This PDF file includes:

Supplementary Texts 1 and 2
Figs. S1 to S10
Table S1
Legends for movies S1 and S2

Other Supplementary Material for this manuscript includes the following:

Movies S1 and S2

REFERENCES AND NOTES

1. P. Kannus, Structure of the tendon connective tissue. *Scand. J. Med. Sci. Sports* **10**, 312–320 (2000).
2. C. N. Maganaris, J. P. Paul, Hysteresis measurements in intact human tendon. *J. Biomech.* **33**, 1723–1727 (2000).
3. D. R. King, Macroscale double networks: Highly dissipative soft composites. *Polym. J.* **54**, 943–955 (2022).
4. I.-C. Liao, F. T. Moutos, B. T. Estes, X. Zhao, F. Guilak, Composite three-dimensional woven scaffolds with interpenetrating network hydrogels to create functional synthetic articular cartilage. *Adv. Funct. Mater.* **23**, 5833–5839 (2013).
5. W. R. K. Illeperuma, J.-Y. Sun, Z. Suo, J. J. Vlassak, Fiber-reinforced tough hydrogels. *Extreme Mech. Lett.* **1**, 90–96 (2014).
6. C. Mo, H. Long, J. R. Raney, Tough, aorta-inspired soft composites. *Proc. Natl. Acad. Sci. U.S.A.* **119**, e2123497119 (2022).
7. D. R. King, T. L. Sun, Y. Huang, T. Kurokawa, T. Nonoyama, A. J. Crosby, J. P. Gong, Extremely tough composites from fabric reinforced polyampholyte hydrogels. *Mater. Horiz.* **2**, 584–591 (2015).
8. S. Lin, C. Cao, Q. Wang, M. Gonzalez, J. E. Dolbow, X. Zhao, Design of stiff, tough and stretchy hydrogel composites via nanoscale hybrid crosslinking and macroscale fiber reinforcement. *Soft Matter* **10**, 7519–7527 (2014).
9. H. Yang, M. Ji, M. Yang, M. Shi, Y. Pan, Y. Zhou, H. J. Qi, Z. Suo, J. Tang, Fabricating hydrogels to mimic biological tissues of complex shapes and high fatigue resistance. *Matter* **4**, 1935–1946 (2021).
10. X. Liu, J. Wu, K. Qiao, G. Liu, Z. Wang, T. Lu, Z. Suo, J. Hu, Topoarchitected polymer networks expand the space of material properties. *Nat. Commun.* **13**, 1622 (2022).
11. N. A. Kotov, I. Dekany, J. H. Fendler, Layer-by-layer self-assembly of polyelectrolyte-semiconductor nanoparticle composite films. *J. Phys. Chem.* **99**, 13065–13069 (1995).

12. P. Podsiadlo, A. K. Kaushik, E. M. Arruda, A. M. Waas, B. S. Shim, J. Xu, H. Nandivada, B. G. Pumplin, J. Lahann, A. Ramamoorthy, N. A. Kotov, Ultrastrong and stiff layered polymer nanocomposites. *Science* **318**, 80–83 (2007).
13. M. Rubinstein, R. H. Colby, in *Polymer physics* (Oxford University Press, 2003).
14. C. Fernández-Rico, T. Sai, A. Sicher, R. W. Style, E. R. Dufresne, Putting the squeeze on phase separation. *JACS Au* **2**, 66–73 (2022).
15. T. L. Sun, T. Kurokawa, S. Kuroda, A. B. Ihsan, T. Akasaki, K. Sato, M. A. Haque, T. Nakajima, J. P. Gong, Physical hydrogels composed of polyampholytes demonstrate high toughness and viscoelasticity. *Nat. Mater.* **12**, 932–937 (2013).
16. S. R. Stauffer, N. A. Peppast, Poly(vinyl alcohol) hydrogels prepared by freezing-thawing cyclic processing. *Polymer* **33**, 3932–3936 (1992).
17. M. Hua, S. Wu, Y. Ma, Y. Zhao, Z. Chen, I. Frenkel, J. Strzalka, H. Zhou, X. Zhu, X. He, Strong tough hydrogels via the synergy of freeze-casting and salting out. *Nature* **590**, 594–599 (2021).
18. X. Hu, M. Vatankhah-Varnoosfaderani, J. Zhou, Q. Li, S. S. Sheiko, Weak hydrogen bonding enables hard, strong, tough, and elastic hydrogels. *Adv. Mater.* **27**, 6899–6905 (2015).
19. G. Zhang, J. Kim, S. Hassan, Z. Suo, Self-assembled nanocomposites of high water content and load-bearing capacity. *Proc. Natl. Acad. Sci. U.S.A.* **119**, e2203962119 (2022).
20. J. Kim, G. Zhang, M. Shi, Z. Suo, Fracture, fatigue, and friction of polymers in which entanglements greatly outnumber cross-links. *Science* **374**, 212–216 (2021).
21. L. Andreozzi, V. Castelvetro, M. Faetti, M. Giordano, F. Zulli, Rheological and thermal properties of narrow distribution poly(ethyl acrylate)s. *Macromolecules* **39**, 1880–1889 (2006).
22. J.-Y. Sun, X. Zhao, W. R. K. Illeperuma, O. Chaudhuri, K. H. Oh, D. J. Mooney, J. J. Vlassak, Z. Suo, Highly stretchable and tough hydrogels. *Nature* **489**, 133–136 (2012).
23. J. P. Gong, Y. Katsuyama, T. Kurokawa, Y. Osada, Double-network hydrogels with extremely high mechanical strength. *Adv. Mater.* **15**, 1155–1158 (2003).
24. J. P. Gong, Why are double network hydrogels so tough? *Soft Matter* **6**, 2583–2590 (2010).
25. T. Finni, J. Peltonen, L. Stenroth, N. J. Cronin, Viewpoint: On the hysteresis in the human Achilles tendon. *J. Appl. Physiol.* **114**, 515–517 (2013).
26. C. Yang, T. Yin, Z. Suo, Polyacrylamide hydrogels. I. Network imperfection. *J. Mech. Phys. Solids* **131**, 43–55 (2019).
27. J. Liu, C. Yang, T. Yin, Z. Wang, S. Qu, Z. Suo, Polyacrylamide hydrogels. II. Elastic dissipater. *J. Mech. Phys. Solids* **133**, 103737 (2019).
28. Y. Zhou, J. Hu, P. Zhao, W. Zhang, Z. Suo, T. Lu, Flaw-sensitivity of a tough hydrogel under monotonic and cyclic loads. *J. Mech. Phys. Solids* **153**, 104483 (2021).
29. M. K. Beyer, The mechanical strength of a covalent bond calculated by density functional theory. *J. Chem. Phys.* **112**, 7307–7312 (2000).
30. W. Zhang, S. Zou, C. Wang, X. Zhang, Single polymer chain elongation of poly(*N*-isopropylacrylamide) and poly(acrylamide) by atomic force microscopy. *J. Phys. Chem. B* **104**, 10258–10264 (2000).
31. M. Tao, S. Lavoie, Z. Suo, M. K. Cameron, The effect of scatter of polymer chain length on strength. *Extreme Mech. Lett.* **61**, 102024 (2023).
32. M.-C. Choi, J.-Y. Jung, H.-S. Yeom, Y.-W. Chang, Mechanical, thermal, barrier, and rheological properties of poly(ether-block-amide) elastomer/organoclay nanocomposite prepared by melt blending. *Polym. Eng. Sci.* **53**, 982–991 (2013).
33. J. Madsen, S. P. Armes, (Meth)acrylic stimulus-responsive block copolymer hydrogels. *Soft Matter* **8**, 592–605 (2012).
34. G. Kocak, C. Tuncer, V. Bütün, pH-responsive polymers. *Polym. Chem.* **8**, 144–176 (2017).
35. H. Kamata, Y. Akagi, Y. Kayasuga-Kariya, U.-I. Chung, T. Sakai, "Nonswellable" hydrogel without mechanical hysteresis. *Science* **343**, 873–875 (2014).
36. J. Rault, A. Lucas, R. Neffati, M. Monleón Pradas, Thermal transitions in hydrogels of poly(ethyl acrylate)/poly(hydroxyethyl acrylate) interpenetrating networks. *Macromolecules* **30**, 7866–7873 (1997).
37. G. G. Ferrer, M. S. Sánchez, J. L. G. Ribelles, F. J. R. Colomer, M. M. Pradas, Nanodomains in a hydrophilic–hydrophobic IPN based on poly(2-hydroxyethyl acrylate) and poly(ethyl acrylate). *Eur. Polym. J.* **43**, 3136–3145 (2007).
38. M. Salmerón Sánchez, G. G. Ferrer, M. Monleón Pradas, J. L. Gómez Ribelles, Influence of the hydrophobic phase on the thermal transitions of water sorbed in a polymer hydrogel based on interpenetration of a hydrophilic and a hydrophobic network. *Macromolecules* **36**, 860–866 (2003).
39. J. L. Gómez Ribelles, M. Monleón Pradas, G. Gallego Ferrer, N. Peidro Torres, V. Pérez Giménez, P. Pissis, A. Kyritsis, Poly(methyl acrylate)/poly(hydroxyethyl acrylate) sequential interpenetrating polymer networks. Miscibility and water sorption behavior. *J. Polym. Sci. B Polym. Phys.* **37**, 1587–1599 (1999).

Acknowledgments

Funding: This work was supported by MRSEC (DMR-2011754) and by the Air Force Office of Scientific Research (FA9550-20-1-0397). J.S. was supported by the NSF Graduate Research Fellowship (DGE1745303). J.K. was supported by Kwanjeong Lee Chonghwan Educational Foundation of Korea (KEF-2017). **Author contributions:** G.Z. conceived the project. G.Z., J.S., J.K., and Z.S. designed the study and interpreted the results. G.Z., J.S., J.K., and C.H.A. conducted the experiments. G.Z., J.S., and Z.S. wrote the manuscript. Z.S. supervised the research. All authors discussed the result and commented on the manuscript. **Competing interests:** The authors declare that they have no competing interests. **Data and materials availability:** All data needed to evaluate the conclusions in the paper are present in the paper and/or the Supplementary Materials.

Submitted 19 March 2023
Accepted 26 May 2023
Published 30 June 2023
10.1126/sciadv.adh7742